

Laser-Based Non-Destructive Detection of Inner Flaws in Concrete with the Use of Lamb Waves

Oleg KOTYAEV, Yoshinori SHIMADA, Kazuhisa HASHIMOTO, Institute for Laser Technology, Osaka-fu, Japan

Abstract. A laser system for remote non-destructive inspection of concrete structures has been developed. The system is intended for the location of inner flaws in concrete structures, mainly in concrete transportation tunnels. The technique is based on the initiation and detection of Lamb waves and ultrasonic vibration in concrete with the use of a laser photorefractive interferometer. Vibration in concrete is initiated by laser impact provided by a pulsed Nd:YAG laser operating at wavelength of 1064 nm. A CW Nd:YAG laser radiation of 532 nm wavelength is used for detection. The laser interferometer uses principles of dynamic holography via two-wave mixing in photorefractive crystal and homodyne detection. A photorefractive crystal – Bismuth Silicon Oxide (BSO) – is used as a nonlinear medium for the recording of the dynamic hologram. Concrete samples used in the laboratory experiments reproduce real concrete material used in transportation tunnels. Various types of inner defects like voids, cracks and honeycombs have been tested. Lamb waves initiated by laser impact are detected by the interferometer. Analysis of Lamb wave spectra provides information of defect location. Accuracy of location is about 2 cm. A mobile model of the system has been assembled and demonstrated in field conditions.

Introduction.

Accident prevention is one of the most important conditions of providing safe transportation. However, in spite of taking safety measures, sometimes accidents happen suddenly. In October 1999, Mainichi Shimbun (Tokyo) reports a giant 226-kilogram concrete chunk fell from the wall of a tunnel on the Sanyo Shinkansen Line, stopping bullet train services on the line and stranding thousands of passengers. The original block was 3.3 meters long, 40 centimeters wide and 15 centimeters thick (Figure 1). Fortunately, there was no train that time in the tunnel. No one was injured and nothing else was damaged. However, this fact shows that it is impossible to guarantee 100% safety in bullet train transportation. After the accident, the JR West Company inspected 142 tunnels and found 2,049 points with faults where concrete was not properly attached to the tunnels.

Development of reliable inspection technique still remains one of the most important tasks. The JR West tunnels were inspected with the use of conventional contact methods like hammering and piezo-sensing (Figure 2). However, it is believed that there exists more promising technique: laser based inspection can provide real remote inspection with acceptable sensitivity, insensibility to surface roughness and high operation rate.

Laser-based detection of vibration is a technique for remote non-destructive inspection, in which a pulsed laser is used to generate a sound wave and a CW laser is used for detection [1].



Fig. 1. A giant concrete chunk fell from the wall of a tunnel.

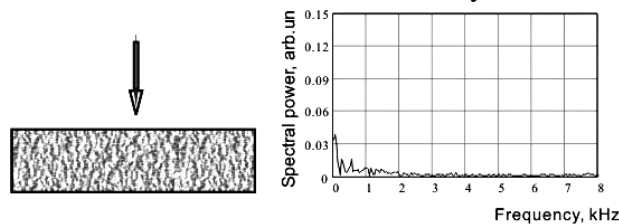


Fig. 2. The JR West Company inspected 142 tunnels and found 2,049 points with faults.

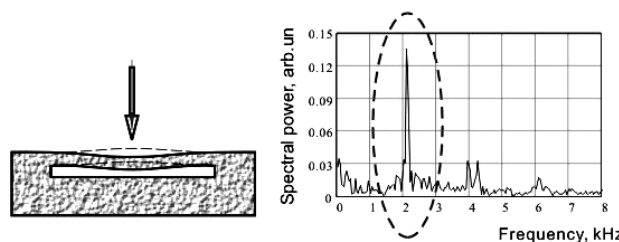
The most commonly used detection device is a laser interferometer, where interference between high quality reference beam and radiation scattered by vibrating concrete surface is analyzed. In our opinion the preferable approach should be based on two-wave mixing process in photorefractive material and homodyne detection of phase modulation [2, 3]. In contrast to conventional interferometers, the technique can operate effectively with the speckled signal which occurs after scattering by concrete surface, because there is no wave front mismatching between interfering signals. In the present report, a prototype of laser system for remote inspection of concrete structures is described.

1. Principle of operation.

The first version of the laser-based system for non-destructive testing of concrete structures



Impact/detection position is over no-defect area.
No visible Lamb wave is initiated.

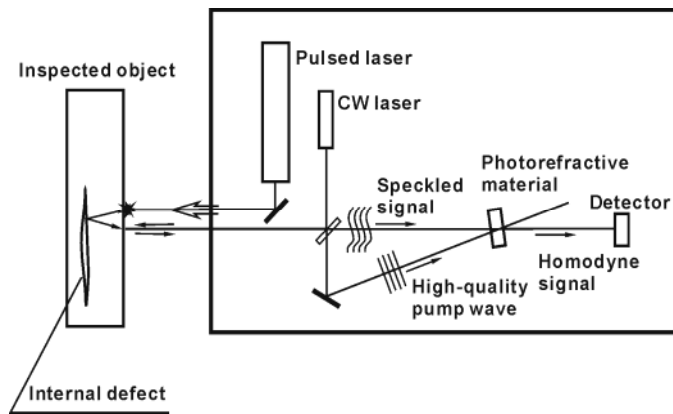


Impact/detection position is over defect.
Lamb wave with frequency of 2.1 kHz is initiated.

Fig.3. Presence of standing Lamb wave is a criterion of the presence of inner flaw.

is supposed to use standing Lamb wave initiation and detection. Principle of testing is very simple. A pulsed laser produces an impact in the inspected object. If concrete quality is good in the inspected area (local concrete layer is thick), no detectable Lamb wave is initiated. However, if the impact position takes place over defect area, a standing Lamb wave is initiated (Figure 3), and it can be detected with the use of photorefractive interferometer. So, the criterion of the presence/absence of inner defect is appearance of initiated standing Lamb wave.

Schematic diagram of the detection technique is shown in Figure 4. Output CW laser beam is split into two beams: high quality pump beam



(used as a reference beam) and probe beam illuminating the inspected surface. Forming optical system produces the probe beam focused on the inspected surface. The same optical system collects radiation scattered by the inspected surface. This signal and the pump beam intersect each other in a photorefractive crystal and record a dynamic hologram [4, 5].

Fig. 4. Principle of operation.

When the pump beam reads the hologram, a diffracted beam appears in the direction of the transmitted signal beam. The main benefit of using the dynamic hologram is absence of wave front mismatch between the speckled signal and diffracted pump wave. Resulting effective interference between monochromatic pump wave and phase-modulated signal leads to the conversion of phase modulation into an amplitude modulation.

The resulting homodyne signal is detected by a photodetector. Both spectra and waveform of the signal can be easily analyzed providing information of quality of inspected concrete structures.

The main application of the first version of the system is the inspection of transportation tunnels.

2. Experimental Conditions.

2.1. Experimental setup.

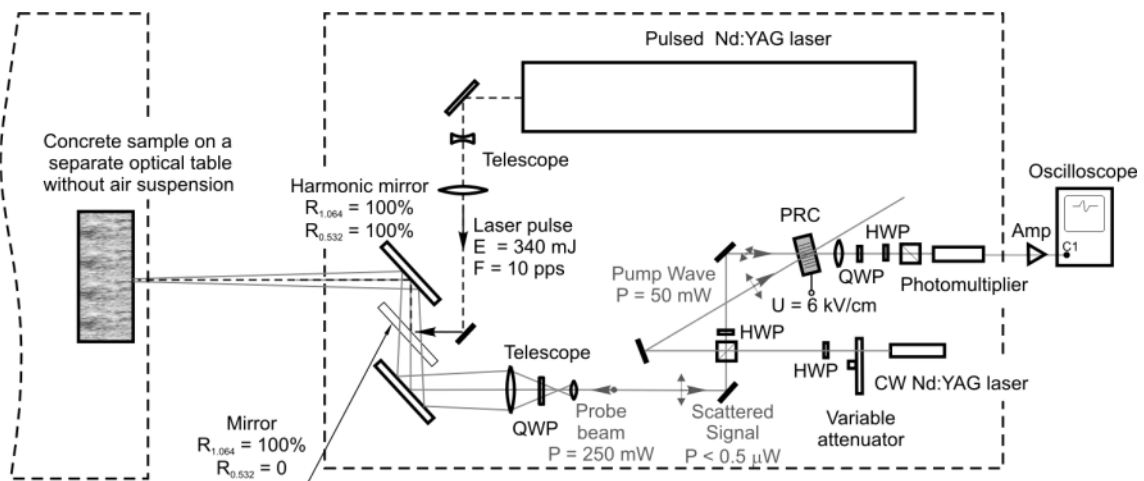


Fig.5. Schematic diagram of laboratory experimental setup.
 PRC – photorefractive crystal, QWP and HWP – quarter- and half-wave plates.

Schematic diagram of the experimental setup is shown in Figure 5. Pulsed Nd:YAG laser produces laser impact beam. In the experiments, the weak ablation mode of laser impact is used. Impact energy is 340 mJ. Impact beam size is about 4 mm, producing laser peak intensity of 270 MW/cm^2 . Pulse repetition rate is 10 pps. To average the recorded waveform and increase signal-to-noise ratio (SNR), 15÷50-shot series are used.

A CW Nd:YAG laser at the second harmonic is used for detection of initiated Lamb waves. Output radiation is split into two beams: the pump beam with power of 50 mW and the probing beam with power of 250 mW. Probing beam is focused on the sample surface. Power of radiation scattered by concrete and used as a working signal does not exceed 0.5 μ W.

The pump beam and scattered signal record a dynamic hologram in the BSO photorefractive crystal (PRC) and produce the homodyne signal which is detected by a photomultiplier tube and analyzed by an oscilloscope. The PRC is used in the drift mode. Applied electric field strength is 6 kV/cm.

In the experiments, the surface of concrete samples is scanned by impact and probing beams. Direction of both beams is controlled by a single harmonic mirror simultaneously. Distance between impact and probe beams is 5 mm. Both beams scan the surface of a sample from its center to edge with 1 cm steps.

To isolate the interferometer from any external sources of vibration, an optical table with air suspension is used. However, inspected samples are installed on a separate table without any air suspension corresponding to field condition. Distance between concrete surface and the interferometer is about 1.5 m.

2.2. Concrete samples used in the experiments.

The samples used in the experiments are made form concrete which is actually used in the transportation tunnels in Japan. We have ordered from JR West Company five samples with different defects (Figure 6). All of the samples are 30×30×10 cm concrete plates. One sample has no defect inside. And four samples have inner void, crack and honeycomb defects.

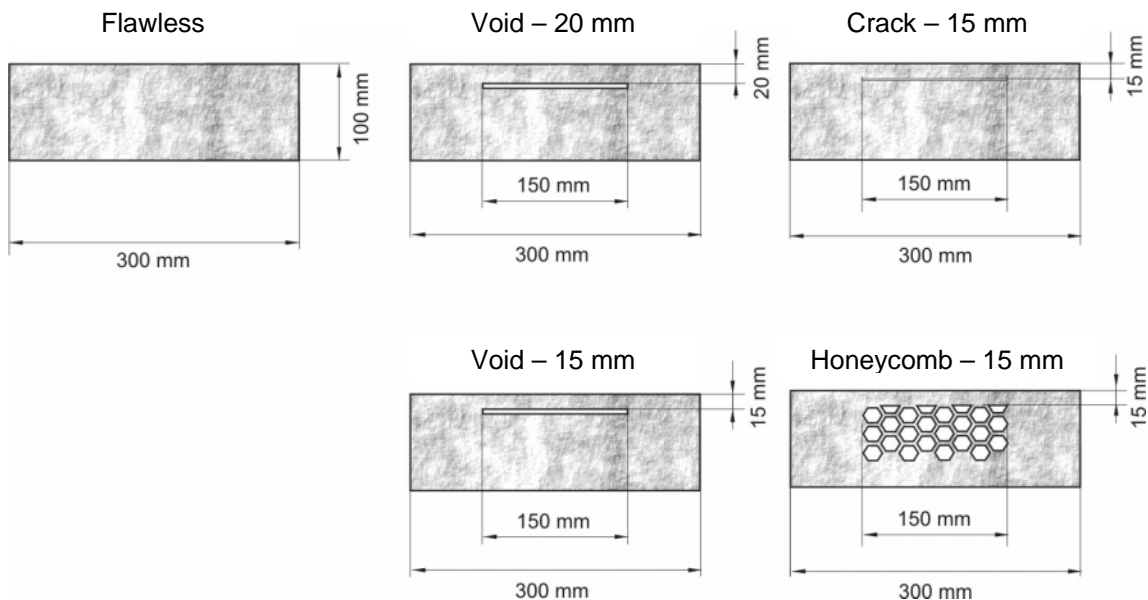


Fig.6. Details of the concrete samples.

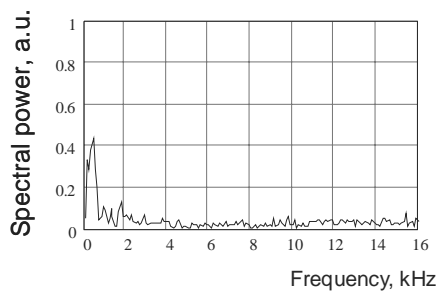


Fig. 7. The flawless sample. As it was expected, no detectable Lamb wave has been initiated.

frequency noise around 0.5 kHz takes place. Absence of detectable Lamb wave verifies that the sample is really flawless.

Inspection of the defected samples has revealed the different responses. Figure 8 shows typical spectra obtained in the defected samples. The scanning of each sample

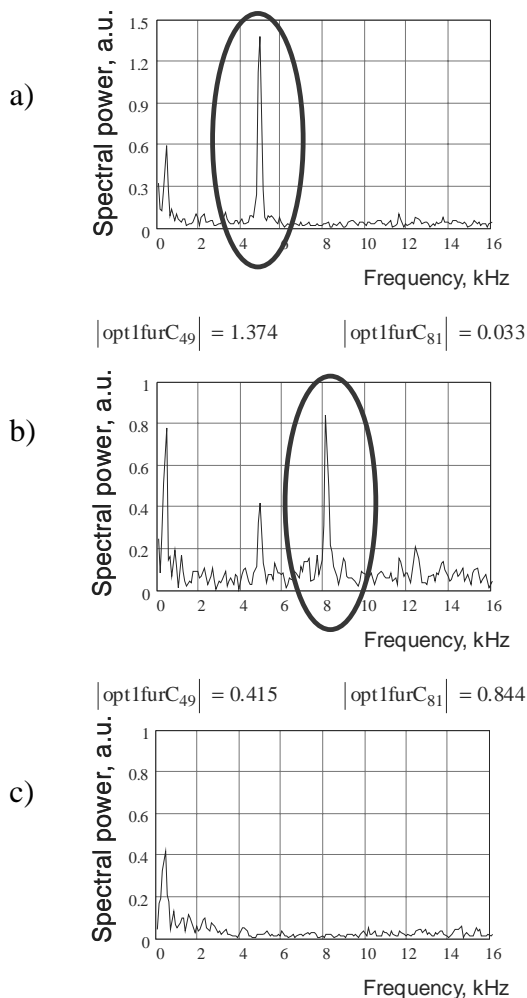


Fig. 8. Sample with the honeycomb defect (15×15 cm, depth – 15 mm). a) impact/probe position: the sample center – the first harmonic (4.9 kHz) is dominant; b) impact/probe position: 4 cm from the sample center – the second harmonic (8.1 kHz) is dominant; c) impact/probe position: 11 cm from the sample center – no detectable Lamb wave is observed.

3. Experimental Results of Inspection of Concrete Samples.

Inspection of the flawless sample has shown that no detectable Lamb wave can be initiated in the sample. In any impact/detection position, spectrum of detected signal looks like one shown in Figure 7. For better visualization, the spectrum is presented in linear scale (a.u. – arbitrary units). One can see that there are no clear peaks in the spectrum. Only low-

frequency noise around 0.5 kHz takes place. Absence of detectable Lamb wave verifies that the sample is really flawless.

surface results in initiation and detection of various modes of Lamb waves. For example, in the sample having a honeycomb defect (Figure 8), central impact/detection position produces the first harmonic of standing Lamb wave (4.9 kHz – Figure 8-a). Moving impact/detection position away from the sample center leads to gradual decrease of the first harmonic power and increase of the second harmonic power. The most powerful second harmonic is initiated when impact/detection position is located in the middle between sample center and the defect edge – about 4 cm from the sample center. Figure 8-b shows that in this position the second harmonic (8.1 kHz) is dominant. When the scanning reaches the defect edge (7.5 cm from the sample center), detectable Lamb waves are no longer initiated. Figure 8-c shows the result of detection when impact/probe position is located over no-defect area: 11 cm from the sample center – no detectable Lamb wave is observed.

Similar behavior of initiated Lamb waves has been observed in the other defected samples. The only difference is frequencies of the harmonics.

The results of the scanning of the defected samples are presented in Figures 9 ÷ 12. Each figure shows the distribution of Lamb wave spectral power over sample surface when scanning from its center towards its edge. Solid lines represent the first harmonics, dotted lines – the second harmonics.

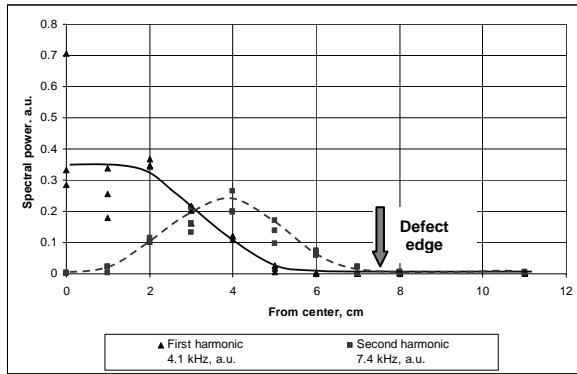


Fig. 9. Sample with the VOID (depth – 20 mm). Detection accuracy is about 1 cm.

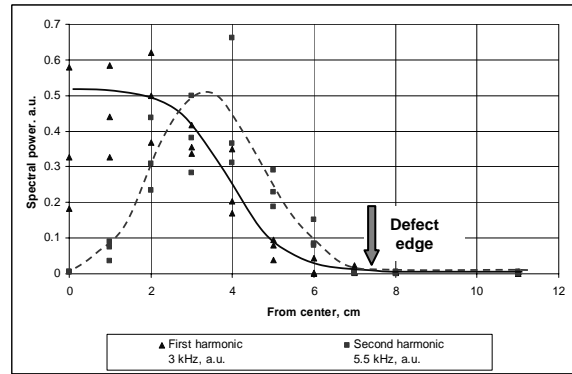


Fig. 10. Sample with the VOID (depth – 15 mm). Detection accuracy is about 1 cm.

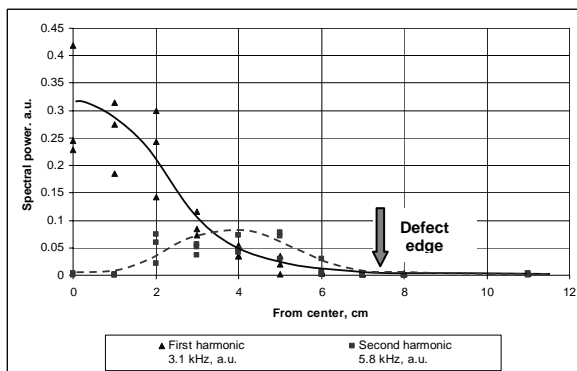


Fig. 11. Sample with the CRACK (depth – 15 mm). Detection accuracy is about 2 cm.

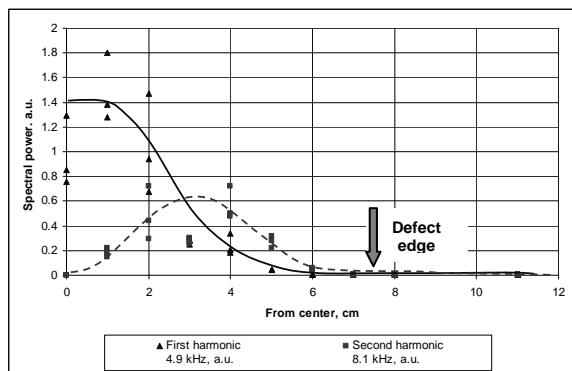


Fig. 12. Sample with the HONEYCOMB defect (depth – 15 mm). Detection accuracy is about 2 cm.

Table 1. Summary of the inspection results.				
#	Sample description.	First harmonic, kHz	Second harmonic, kHz	Accuracy of flaw detection
	All samples – 30×30×10 cm plates			
1	Flawless	-	-	-
2	VOID, depth – 20 mm	4.1	7.4	1 cm
3	VOID, depth – 15 mm	3.0	5.5	1 cm
4	CRACK, depth – 15 mm	3.1	5.8	2 cm
5	HONEYCOMB, depth – 15 mm	4.9	8.1	2 cm

Accuracy of detection is defined as the distance between the defect edge and impact/detection position when spectral power of the second harmonic reaches about 10% of its maximum.

The table 1 contains summary of the experimental results. Five samples have been tested. One sample is flawless and four samples have various inner defects. Test of the flawless sample has not shown any response, as it was expected. Tests of four samples have demonstrated reliable detection of inner defects with accuracy better than 2 cm.

To verify the defect detection results, transmission of acoustic wave through the samples has been examined. Testing of flawless sample in transmission configuration has not revealed any nontransparent area. However, the defected samples have demonstrated noticeable difference in approaching time of transmitted wave. Propagation through flawless area takes about 28 μs , and the wave bypassing the inner defect becomes visible at 55-th μs after laser impact. That means, acoustic wave propagating through central part of these samples meets some nontransparent structure which does not allow the wave to propagate directly.

As well, additional examination with the use of conventional hammering method and infra-red testing has verified the defect detection results obtained with the use of laser-based system.

Now we can state, that the laser-based system has detected these defects reliably with satisfying accuracy.

A few words about frequency of initiated Lamb waves. As it was expected, frequency depends on defect dimensions and its depth. The deeper defect location (or the thicker concrete layer between defect and sample surfaces) the higher Lamb wave frequency [6]. Samples with void and crack located at the depth of 15 mm have almost similar frequency of the first harmonic of standing Lamb wave: 3 and 3.1 kHz respectively. Sample with the void located at 20 mm depth has 4.1 kHz first harmonic.

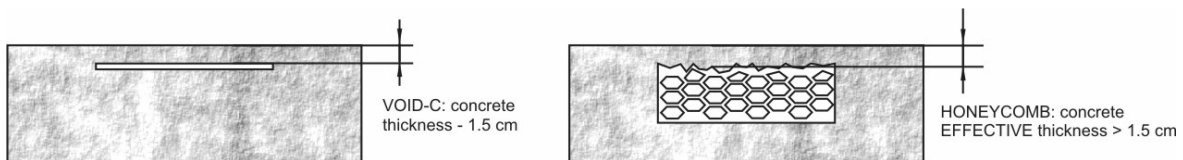


Fig.13. Effective thickness of concrete layer in the samples with honeycomb defect is bigger than in the void sample.

The honeycomb defect is located at the depth of 15 mm, but initiated Lamb wave has higher frequency than samples with void and crack – 4.9 kHz. This fact can be explained by the differences of concrete-defect interface. Voids and cracks are produced by using foam plastic plate and thin plastic film respectively. The honeycomb defect is made from stones and small pieces of concrete. In the honeycomb samples the interface has more irregular shape due to contact between inner side of the front part of the sample and honeycomb stones. Resulting concrete layer between the defect and sample surface is thicker than in the void and crack samples (Figure 13). Initiated Lamb frequency should be higher, as it has been observed in the experiments.

In brief conclusion, we can say that in the experiments, all defects of concrete samples have been detected: voids, cracks and honeycombs. The use of laser-based system has demonstrated reliable detection of initiated Lamb wave which contains information of inner structure of concrete.

Response of defect samples depends on defect transverse dimensions, depth of defect location (or thickness of concrete layer between defect and sample surface) and concrete-defect interface.

The thickness of the defect itself does not matter: voids and cracks having the same dimensions and located at the same depth will respond in one and the same way.

Accuracy of defect location is 2 cm and better. In our opinion it is more than enough for real-time inspection of transportation tunnels.

The laser system of inspection of concrete tunnel is basically ready for the tests in the field conditions.

4. Additional Tests for Preparation to the Field Experiments.

Before going to the real tunnel we explored the field experiment site and performed some additional experiments. We have found the following. The mobile prototype of the laser-based system can be delivered to the experimental site. Parameters of the inner defect in the tunnel allow to consider the defect to be detectable reliably. The system provides satisfying stability of the detected Lamb wave. Energy of impact laser pulse will be enough for Lamb wave initiation. The interferometer sensitivity allows to operate with signals having power more than 10 times lower than in the main laboratory experiments.

Final conclusion: it is feasible to go to the real tunnel for field experiments and test the laser-based system in the real inspection.

5. Test of the Mobile Prototype of the Laser-Based System for Non-Destructive Inspection of Concrete Structures in the Field Conditions.

5.1. The field experimental set-up and experimental conditions.

The mobile prototype of the laser-based system for non-destructive testing of concrete walls was assembled and loaded on a small track (Figure 14). Overall dimensions of the loaded system did not exceed $1 \times 1.5 \times 0.5 \text{ m}^3$. The system was equipped with air-suspension and covered by a plastic box (shown in Figure 15).

The first examination of the laser-based inspection system was taken during the transportation of the system to the experimental site. The old railway sleepers made us to drive very carefully. The track took strong list. Sometimes, the system underwent strong vibration when the track wheels went over the sleepers. All the laser units were on the track. Successful operation test has demonstrated that the system has passed the hard transportation test without any damage; and the system can be considered as reliable in service.

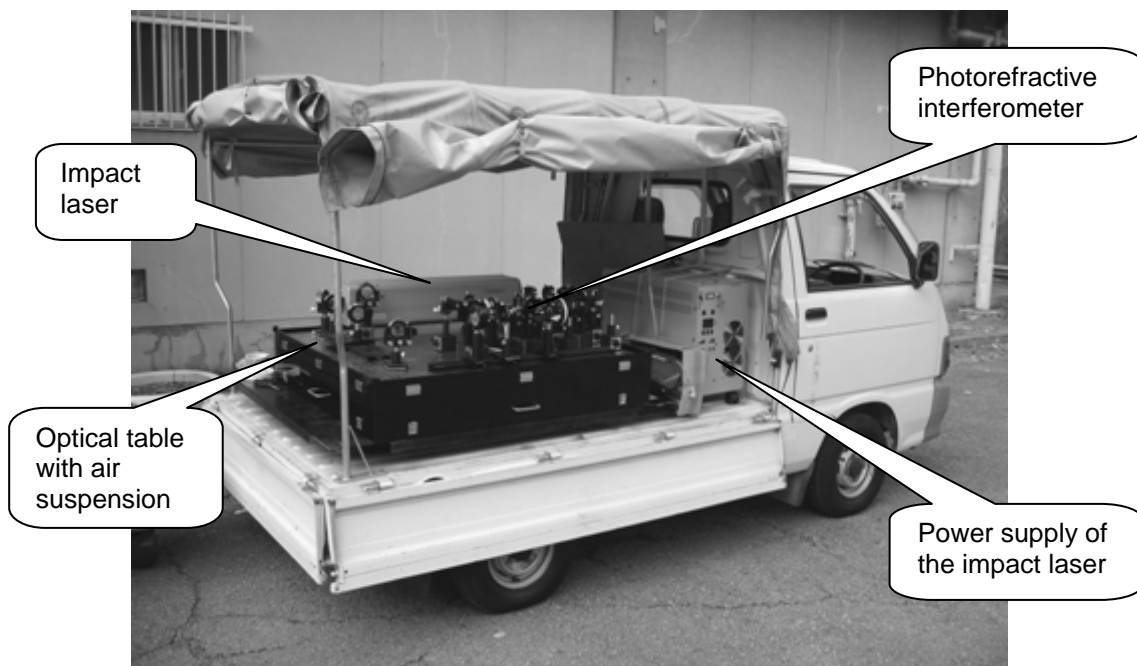


Fig. 14. The laser system is loaded on a small track.

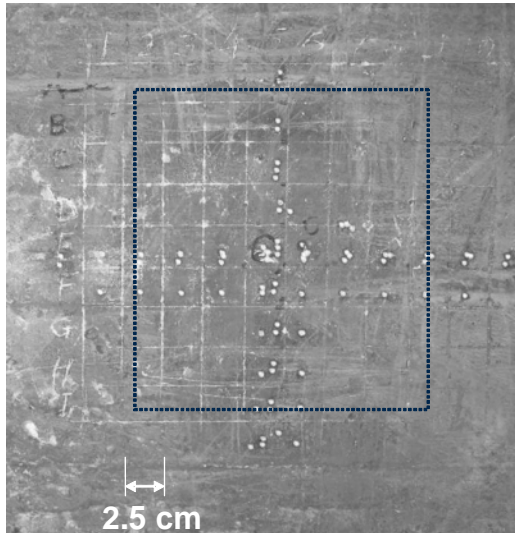


Fig. 15. The defect area. Dotted rectangular – approximate boundaries of the inner flaw detected by light hammering.

directions with 2.5 cm steps. The inspected area completely covered the defect area which had been approximately determined by a light hammer (Figure 15).

Tunnel width, height and length are approximately 4, 5 and 300 m, respectively. The tunnel has no illumination. Sometimes strong wind takes place. To protect our system during the experiments, it was covered by a tent.

Surface of concrete walls in the tunnel differs from surface of concrete samples used in the laboratory experiments. It is dirty, much rougher and much darker. As a result, power of scattered radiation and collected by the interferometer lenses is much lower than in the laboratory experiments. In the tunnel, collected power did not exceed 5 nW.

The operating system is shown on Figure 16. The tent walls have been removed and the box doors have been opened just to get these pictures. The probe beam is clearly seen on the left picture. On the right picture, bright spot on the wall corresponds to current impact/detection position.



Fig. 16. The system is on operation.

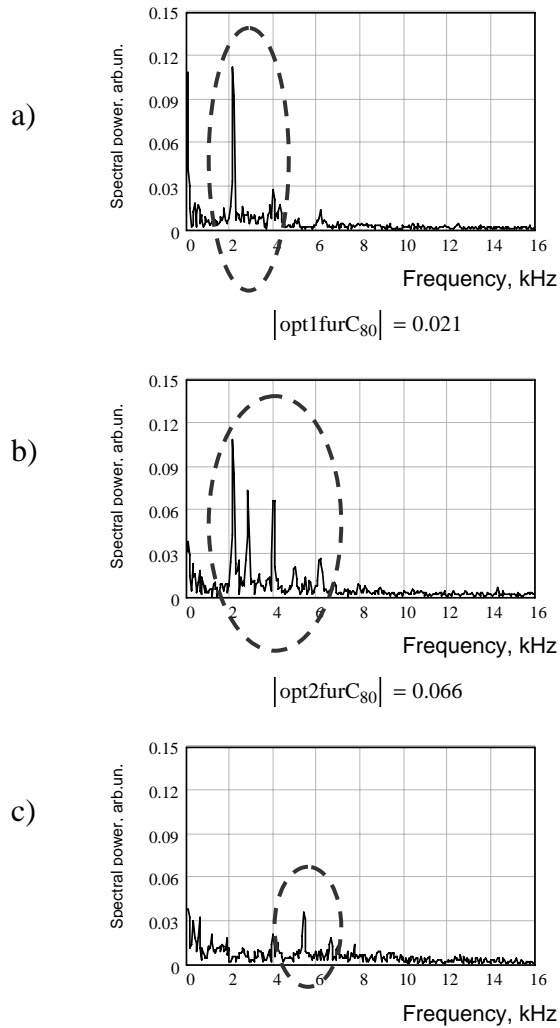


Fig. 17. The results of vertical scanning of the defect area. a) defect center – Lamb wave frequencies 2.1 and 4 kHz; b) 5 cm above the defect center – Lamb wave frequencies 2.1, 2.8, 4 and 6 kHz; c) 10 cm above the defect center – signal at 5.4 kHz – probably defect still exists.

directions. The vertical distribution of spectral power of three modes of standing Lamb wave is shown in Figure 18: solid line represents 2.1 kHz mode, dotted line – 2.8 kHz and punctual line – 4 kHz mode. The total area covered by the spectral power distribution corresponds to the defect area determined by light hammering. Accuracy of detection using these three modes is about 2 cm. However, in reality, detection will not be limited by three first modes. Figure 17-c shows that the defect can be detected using higher mode of Lamb wave even in the area where light hammering is not sensitive. It should be noted again, only the presence/absence of detectable Lamb wave can be a criterion of quality, no matter what mode of Lamb wave is initiated.

The scanning in horizontal direction has shown similar results: many modes of Lamb waves can be initiated; accuracy of defect detection is better than 2 cm.

5.2. Lamb wave initiated in the tunnel wall.

After the system operation test, the tunnel wall in the defect area was examined. In the very first attempt, positive result was obtained: easily and reliably detectable Lamb wave was observed at frequency around 2.1 kHz.

Figure 17 shows typical spectra obtained in the defect area. The scanning of its surface in vertical direction results in initiation and detection of various modes of Lamb wave. Central impact/detection position produces dominant standing Lamb wave at frequency 2.1 kHz (Figure 17-a). Moving impact/detection position away from the defect center leads to gradual redistribution of spectral power to other modes. For example, when impact/detection position is 5 cm above the sample center, Lamb wave with frequency of 2.1 kHz is still dominant; however, peaks at 2.8, 4 and 6 kHz arise (Figure 17-b). When the scanning reaches the defect edge (about 10 cm from the defect center), these modes disappear, and the new mode with 5.4 kHz frequency takes place (Figure 17-c). Probably, concrete layer in this position is comparatively thick, and light hammering was not capable to recognize the real defect boundary.

The entire defect area has been scanned in vertical and horizontal

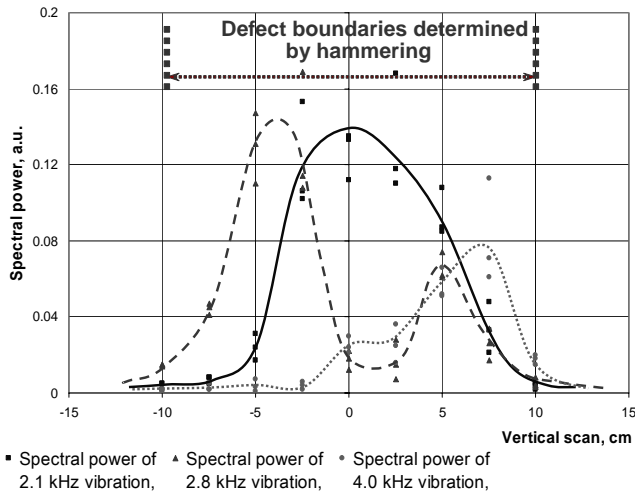


Fig. 18. The defect area – vertical scanning. Distribution of spectral power Lamb wave over the sample surface. The inner flaw can be detected with accuracy of 1.5 cm.

5.3. Conclusions.

The experimental results presented in this paper bring out clearly that the first version of laser-based system for non-destructive inspection of concrete tunnels has demonstrated very promising operation. The mobile prototype of the system has shown reliable capability of detection of inner defect with acceptable accuracy. The detection accuracy obtained with the use of three first modes of Lamb wave corresponds to the detection results obtained with the use of light hammering with 2 cm error, which is more than enough for testing concrete structures. The system

clearly recognizes the questionable zone of concrete wall: real inner defect has been revealed.

Distance of 2.5 m between the system and inspected tunnel wall is only two times shorter than inspection distance in the real transportation tunnel having inner radius of 5 m. Reliable detection at 2.5 m distance makes it clear that the system has practicable potentials in using the system for tunnel inspection.

So, we can state that the principles of the first version of laser-based system for tunnel inspection have been developed; corresponding mobile prototype has been successfully tested in the field conditions. The next step is development of industrial design, manufacturing and putting the system in real operation. More compact design of the interferometer, more energetic impact laser and more powerful detection laser, effective scanning unit, algorithm of data logging and processing with corresponding software – all these things are the matter of further steps.

References

- [1] P.Delays, A.Blouin, L.-A.Montmorillon, D.Drolet, J.-P.Monchalain, and G.Roosen, "Photorefractive detection of ultrasound", Proceedings of SPIE, 3137 (1997), pp. 171-182.
- [2] M.B.Klein, G.D.Basher, A.Grunnet-Jepsen, D.Wright, and W.E.Moerner, "Homodyne detection of ultrasonic surface displacement using two-wave mixing in photorefractive polymers", Proceedings of SPIE, 3589 (1999), pp. 22-29.
- [3] Blouin, P.Delays, D.Drolet, and J.-P.Monchalain, "Optical detection of ultrasound by two-wave mixing in photorefractive semiconductor crystals under applied field", Rev. of Progress in Quantitative Nondestructive Evaluation, 16 (1997), pp. 571-577.
- [4] P.Yeh, Introduction to photorefractive nonlinear optics, John Wiley & Sons, Inc., NY, 1993
- [5] R.K.Ing and J.-P.Monchalain, "Broadband optical detection of ultrasound by two-wave mixing in a photorefractive crystal", Appl.Phys.Lett. 59 (1991), pp. 3233-3235
- [6] M.J. Sansalone and W.B.Streett, Impact-echo. Nondestructive evaluation of concrete and masonry. Bullbrief Press, Ithaca, N.Y, 1997.